Journal of Molecular Catalysis B: Enzymatic 59 (2009) 116–120

Contents lists available at ScienceDirect

Journal of Molecular Catalysis B: Enzymatic

journal homepage: www.elsevier.com/locate/molcatb

Lipase entrapment in a zirconia matrix: Sol–gel synthesis and catalytic properties

Domenico Pirozzi[a,*], Esther Fanelli[b], Antonio Aronne[b], Pasquale Pernice[b], Alessio Mingione[a]

[a] Dipartimento di Ingegneria Chimica, Università di Napoli Federico II, P.le Tecchio,80-80125–Napoli, Italy
[b] Dipartimento di Ingegneria dei Materiali e della Produzione, Università di Napoli Federico II, P.le Tecchio,80-80125–Napoli, Italy

ARTICLE INFO

Article history:
Received 7 July 2008
Received in revised form 28 January 2009
Accepted 30 January 2009
Available online 10 February 2009

Keywords:
Lipase
Zirconia
Sol–gel
Biocatalysts
Biomaterials

ABSTRACT

Zirconia-based sol–gels have been used for lipase entrapment, to avoid the biocatalyst inactivation associated to the use of basic or acid catalysts. The method developed allows a single-step entrapment of the enzyme in a zirconia sol–gel with mesopores of diameter in the range 2–4 nm, and a surface area of 219 $m^2\ g^{-1}$. The zirconia matrix is substantially unaffected by the presence of the lipase. The size of the pores, though smaller than that of the enzyme, seems large enough to minimise the effect of the internal diffusional limitations on the overall reaction kinetics, as demonstrated by the substantial equivalence between the activation energies measured with the free and with the immobilised lipase. The thermal inactivation of the zirconia-entrapped lipase, characterised by a mathematical model, is significantly reduced as compared to the inactivation of the free enzyme.

1. Introduction

Sol–gel nanomaterials are gaining a growing importance as solid supports for the immobilisation of biomolecules to be used for biocatalysis, biosensors, and biomedical applications, offering a useful alternative to the traditional polymer technology [1–5]. As a matter of fact, thanks to their porous structure in nanometer dimensions, sol–gel materials offer unique intrinsic properties, such as high surface to volume ratio, large surface area and porosity. In addition, the sol–gel process offers higher flexibility as regards the surface, composition and properties. Furthermore, nanoporous materials, especially inorganic nanoporous materials, which are made mostly of metal oxides, are usually nontoxic, inert, chemically and thermally stable, so they have wide applications where biocompatibility and thermal stability requirements are essential.

Due to the low temperature processing, the sol–gel technology offers useful methods to immobilise heat-sensitive biomolecules. Nevertheless, the structure/activity of encapsulated biomolecules could be affected by the presence of enzyme-denaturing and cytotoxic alcohol in the reaction media, both as cosolvents or as products of the hydrolysis/condensation reactions. In addition, when carrying out the synthesis of silica sol–gel materials, such reactions are usually too slow and need basic or acid catalysis, causing extreme pH values, giving rise to biocatalysts inactivation.

In this study, the entrapment of lipases in zirconia-based sol–gel material has been undertaken to improve the enzyme stability. The sol–gel method allowed to make the support material and to entrap the enzyme in a single step, starting from a solution containing both the matrix precursors and the enzyme, so that when the gelation occurs the enzyme remains entrapped and uniformly dispersed in the gel. Moreover, due to high hydrolysis and polycondensation rates offered by zirconia precursors, a neutral pH could be adopted, avoiding any possible configurational modification of the enzyme induced by acid or basic environments.

So far, zirconia has been used as a support for enzyme immobilisation only in the form of a zirconia/nafion composite [6,7], obtained by casting on an electrode a solution containing zirconia, nafion and an enzyme.

Lipases, chosen as model enzyme, are used in a growing number of industrial applications, both in aqueous and in nonaqueous media. In particular, immobilised lipases have been successfully used in organic synthesis [8–10]. Also, lipases have been recently used in biosensors for the determination of lipids for clinical purpose [11,12], and in biosensing [13,14]. So far, immobilisation of lipases by the sol–gel technique has been carried out only using silica-based materials [2,15–18].

2. Experimental

2.1. Enzyme encapsulation in sol–gel material

In a typical test, 45.0 mg of lipase from Rhizopous oryzae and 15 mg of PEG (MW 1450) were dissolved in 3.0 mL of distilled water and the mixture was stirred by hand up to obtaining a clear

* Corresponding author. Tel.: +39 081 7682284; fax: +39 081 2391800.
E-mail addresses: dpirozzi@unina.it (D. Pirozzi), efanelli@unina.it (E. Fanelli), anaronne@unina.it (A. Aronne), pernice@unina.it (P. Pernice).

1381-1177/$ – see front matter © 2009 Elsevier B.V. All rights reserved.
doi:10.1016/j.molcatb.2009.01.010

Nomenclature

a	specific activity of the total enzyme
a_N	specific activity of the native enzyme, N
a_X	specific activity of the partially inactivated form of the enzyme, X
A, B	mathematical constants
D	completely inactivated form of the enzyme
k, k_1, k_2	first order inactivation constants
N	native form of the enzyme
[N]	concentration of the native form of the enzyme, N
t	time
X	partially inactivated form of the enzyme
[X]	concentration of the partially inactivated form of the enzyme

solution. Subsequently, 2.0 mL of supernatant were drawn and added to 8.5 mL of 1-propanol (99.80+%). The resulting solution was added to a solution formed by 10 mL of Zirconium(IV) propoxide (70 wt.% in 1-propanol) and 1.5 mL of acetylacetone (99+%). The final solution was vigorously stirred at room temperature and the gelation occurred in about 20 min. A transparent and homogeneous slightly yellow coloured gel was obtained. The gel was left at room temperature for 3 h and then lyophilized, in vacuum at −50 °C for 20 h. The lyophilized material was washed three times by distilled water to remove the lipase not entrapped. The enzyme concentration in the washing liquid, estimated by the Lowry method [19], was very low, corresponding to a 99% entrapment yield. The measured lipase loading in the biocatalyst was 8.8 mg lipase/g zirconia, whereas the PEG loading was 2.9 mg PEG/g zirconia.

In the same conditions was prepared a zirconia matrix, as reference material both for the activity tests and for surface area measurements. The chemicals were provided by Aldrich, the lipase by Fluka.

2.2. Structure and thermal behaviour

The nature and temperatures of the various reactions occurring during the heating of the biocatalyst and the corresponding weight losses were evaluated by a Netzsch simultaneous thermoanalyser STA 409 PC with Al_2O_3 as reference material. The TG/DTA curves, recorded in N_2 from room temperature up to 900 °C at a heating rate of 10 °C min^{-1}, were carried out on 50 mg of the bulk sample.

The structure of the biocatalyst as well as that of the zirconia matrix were studied by FTIR spectroscopy. FTIR absorption spectra were recorded, in the 4000–400 cm^{-1} range, using a spectrometer equipped with a DTGS KBr (deuterated triglycine sulphate with potassium bromide windows) detector. A spectral resolution of 2 cm^{-1} was chosen. 4.0 mg of each test sample were mixed with 200 mg of KBr in an agate mortar and then pressed into pellets of 13 mm diameter. The spectrum for each sample represents an average of 64 scans, which were corrected for the spectrum of the blank KBr pellet.

2.3. Textural properties

N_2 adsorption–desorption isotherms at −196 °C were obtained by a Micromeritics Gemini II apparatus model 2370. The samples were previously treated at 50 °C for 2 h under N_2 flow. The N_2 adsorption–desorption isotherms were elaborated by the Brunauer–Emmett–Teller (BET) [20] method for the calculation of the surface areas. Pore volumes were determined from the amounts of adsorbed N_2 at $P/P^0 = 0.98$ (desorption curve), assuming the presence of liquid N_2 (density = 0.807 g cm^{-3}) in the pores under these conditions. The pore distribution was evaluated by the Barrett–Joiner–Halenda (BJH) method [20].

2.4. Activity assay

The activity of the immobilised enzyme as well as that of the free enzyme was assayed by monitoring the amount of *p*-nitrophenol released upon hydrolysis of a 0.5 mM solution of *p*-nitrophenyl butyrate (pNPB) in 50 mM of phosphate buffer, usually at pH 7.5. In a typical test, 10 mg of immobilized biocatalyst, 10 mg of ZrO_2 matrix or 0.1 mg of free lipase were added to 2 mL of the reaction mixture. The mixture was incubated in 5 mL test-tubes, using a thermostatic shaker. After the fixed reaction time, the increase in absorbance at 410 nm was measured for 1 min using an apparent extinction coefficient of 1.33×10^4 M^{-1} cm^{-1}. One unit of hydrolase activity was defined as the amount of enzyme or biocatalyst required to transform 1 μmol of *p*-nitrophenyl butyrate to *p*-nitrophenol per min at room temperature.

The catalytic activity of the ZrO_2 matrix was tested to consider the possible contribution to the reaction rate. It appeared to be so low to be neglected in comparison with that of as the biocatalyst and the free enzyme.

2.5. Thermal stability and reusability tests

Operational stability tests on lipases were carried out keeping entrapped or free enzyme samples immersed in 50 mM of phosphate buffer, pH 7.5, at constant temperature. At given deactivation times, enzyme samples were withdrawn and assayed for activity at 37 °C.

Reusability tests on the entrapped lipase were carried out keeping the enzyme samples immersed in 50 mM of phosphate buffer, pH 7.5, at constant temperature for a fixed period (4 days), then removing the lipase from the solution, removing external water with filter paper and keeping it 3 days over silica gel.

3. Results and discussion

3.1. Structural and textural characterisation

TG/DTA curves of biocatalyst bulk sample are displayed in Fig. 1. The overall weight loss given by the TG curve was 44.4 wt.%. The majority of the weight loss takes place from room temperature to about 400 °C. In this range, for a typical gel-derived sample, the evaporation of the solvents and the subsequent pyrolysis and/or

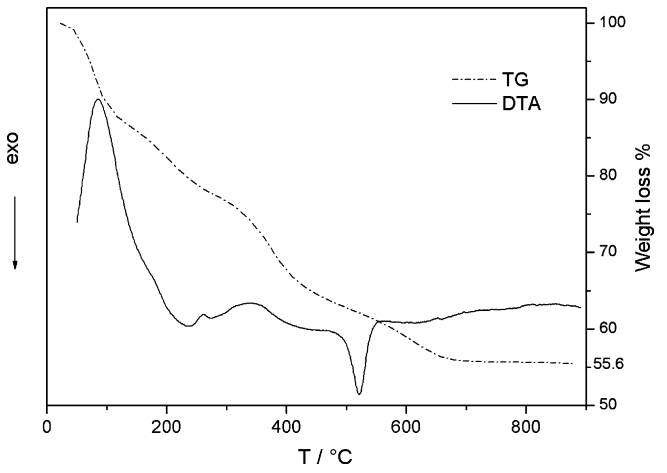

Fig. 1. TG/DTA curves of the zirconia-immobilized lipase, recorded in N_2 at 10 °C min^{-1}.

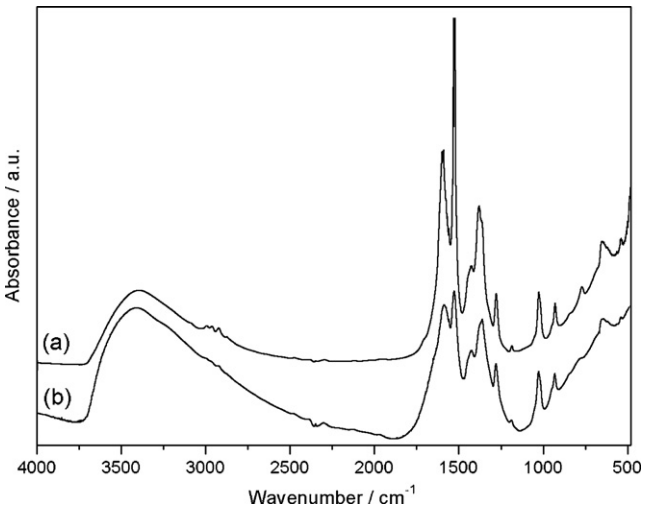

Fig. 2. FTIR spectra of the zirconia-immobilized lipase (a) and zirconia matrix (b).

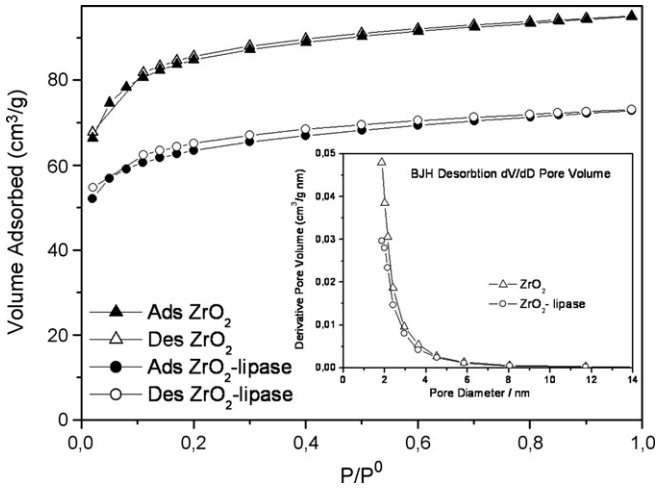

Fig. 3. N_2 adsorption–desorption isotherms of zirconia-immobilized lipase (circles) and zirconia matrix (triangles). In the inset the related pore distribution evaluated by the BJH method is reported.

burning of small molecules generally occur. In the present case, two endothermic peaks are seen in the DTA curve: a high intensity peak centred at 86 °C and a broad low intensity one in the 350–400 °C range. The former can be related to the evaporation from open pores of water and alcohol molecules physically trapped in the gel, the latter to the decomposition of unreacted and strongly bonded molecules. In the 480–650 °C range, a further weight loss is seen with an exothermic peak at 520 °C, indicating that two overlapping phenomena occur: the decomposition of high molecular weight organics such as PEG and lipase and the ZrO_2 crystallization [21].

FTIR spectra of the biocatalyst and of the zirconia matrix are shown in the traces (a) and (b) of Fig. 2, respectively. The spectrum of the zirconia matrix indicates that both residual precursors, solvent and adsorbed water are still present in the sample. Actually, besides the absorption band related to the stretching modes of O—H bonds, 3400 cm^{-1}, the other bands can subdivided in two main groups. The bands lying in the 450–700 cm^{-1} range are related to vibrational modes of the Zr—O bonds in the zirconia network and the ones in the 700–1700 cm^{-1} range to the vibrational modes of the residual 1-propanol and acetylacetone molecules physically adsorbed or coordinated to the zirconia network [22,23].

The FTIR spectrum of the immobilized biocatalyst is very similar to that of the zirconia matrix. No absorption bands related to lipase or PEG are clearly detectable because the majority of them lie in the same range of the other components and more probably because their amount is too small. However the similarity between the two spectra indicates that the presence of lipase does not affect the matrix structure.

N_2 adsorption–desorption isotherms for both zirconia containing lipase and zirconia matrix are reported in Fig. 3. In both cases the isotherms show a gradient over a wide range of P/P° values, suggesting a large contribution of mesopores, despite the absence of any desorption hysteresis. Therefore, the presence of micropores cannot be excluded. The zirconia containing lipase adsorbs a smaller N_2 volume than the zirconia matrix one, showing that in the former sample there is a lower micropores and macropores volume.

The N_2 adsorption data have been elaborated by the BET method, and the corresponding surface areas are reported in Table 1 together with the total pore volume, the micropore volume and the estimated average pore radius. ZrO_2 without enzyme shows high surface area (316 $m^2\ g^{-1}$), whereas the presence of lipase produces a decreasing of the area that keeps still high (219 $m^2\ g^{-1}$). The pore distribution was evaluated by the BJH method (inset of Fig. 3), indicating the presence of mesopores of diameter in the range 2–4 nm. The fact that the lipase diameter (5–7 nm) is substantially larger than the zirconia pore diameter will prevent leaching of the enzyme but may lead to some pore blockage [24–26].

3.2. Catalytic activity

The activity of lipase entrapped in ZrO_2 at 27 °C is 5.43×10^{-7} mmol/($mg_{catalyst}$ min) whereas that pertaining to the free lipase used for the immobilisation is 1.35×10^{-3} mmol/(mg_{lipase} min). As the measured entrapment yield was about 99% (see Section 2), we could estimate the apparent activity of the entrapped lipase to be 5.12×10^{-5} mmol/(mg_{lipase} min). Consequently, the apparent activity of the immobilised enzyme is about 3.8% of the activity of the free enzyme.

The activity-pH profiles of both the free and the immobilised lipases at 27 °C are described in the Fig. 4. In both cases, the catalysts show an optimal pH at about 7.5. The activity of the immobilised enzyme is reported as activity per milligram of catalyst, while that of the free enzyme as activity per milligram of enzyme, and consequently it appears much lower as compared to the activity of the free enzyme.

The Fig. 5 describes the effect of the temperature on the activity of the zirconia-entrapped (Fig. 5a) and free (Fig. 5b) lipase, in the form of an Arrhenius diagram.

The activity of the free lipase is maximum at 35 °C, whereas the optimal temperature for the activity of the entrapped lipase is higher (45 °C). The stabilising effect of the entrapment method is confirmed by the limited inactivation of the entrapped enzyme when the temperature raises over the optimal point. By contrast,

Table 1
Surface area, pore volume and average pore radius of samples of zirconia (with and without lipase) dried at 50 °C.

Sample	BET surface area ($m^2\ g^{-1}$)	Pore volume ($cm^3\ g^{-1}$)	Micropore volume ($cm^3\ g^{-1}$)	Average pore radius r (nm)
ZrO_2	316	0.147	0.081	0.93
ZrO_2–lipase	219	0.113	0.064	1.03

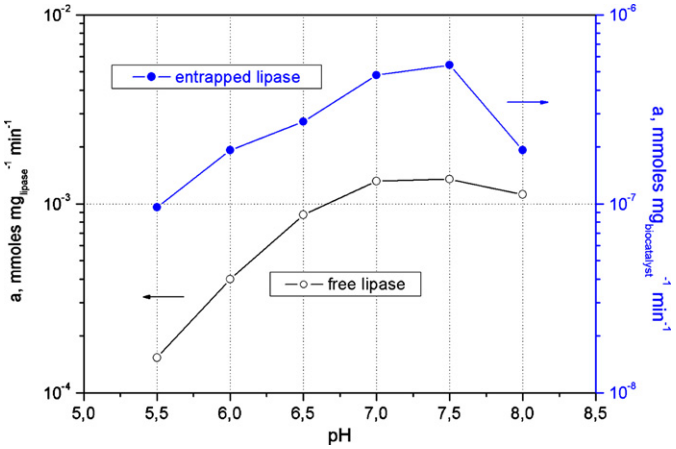

Fig. 4. Effect of pH on the catalytic activity, for the lipase entrapped in zirconia and free lipase dissolved in aqueous solution. The activity of the immobilised enzyme is reported as activity per milligram of immobilized lipase/zirconia system, while that of the free enzyme as activity per milligram of enzyme.

the free enzyme undergoes a significant drop when temperatures higher than 35 °C are adopted.

The activation energy of both the free and the immobilised enzyme have been evaluated by nonlinear regression taking into account only the linear parts of the Arrhenius profiles (dashed lines in Fig. 5a and b). The activation energy of the entrapped lipase

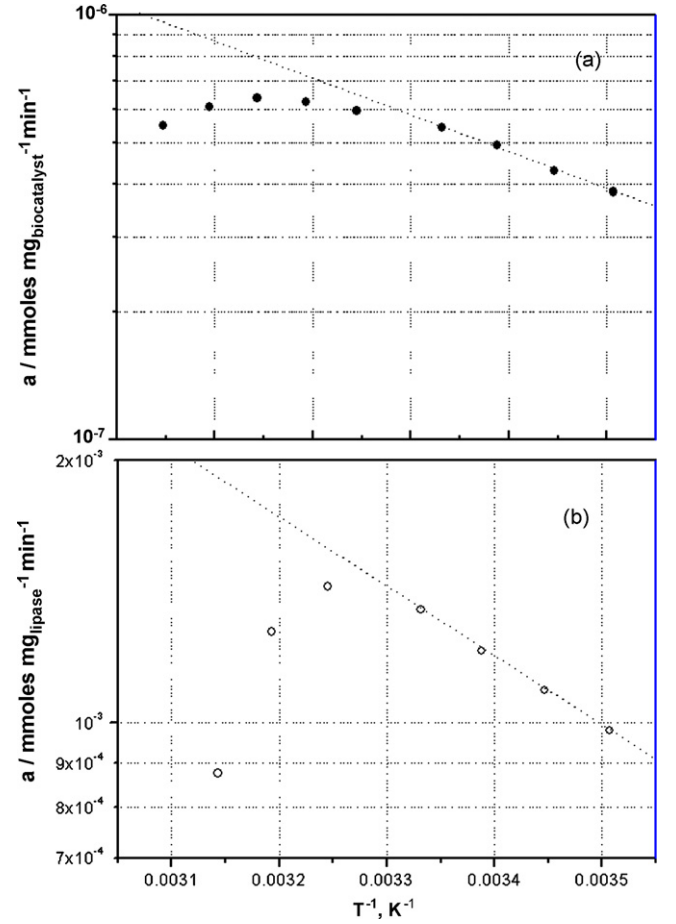

Fig. 5. Effect of temperature on the catalytic activity, for: (a) lipase entrapped in zirconia; (b) free lipase dissolved in aqueous solution. The activity of the immobilised enzyme is reported as activity per milligram of immobilized lipase/zirconia system, while that of the free enzyme as activity per milligram of enzyme.

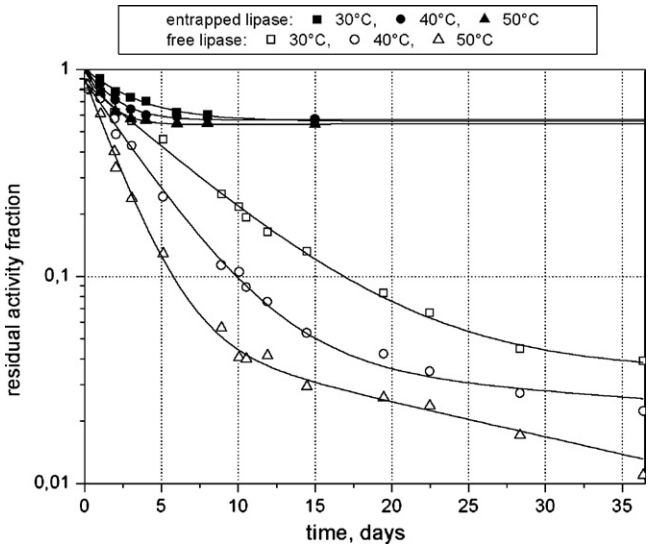

Fig. 6. Thermal inactivation of zirconia-entrapped and free lipases.

(3610 cal mol^{-1}) is not significantly different from that pertaining to the free enzyme (4047 cal mol^{-1}). These results suggest that the overall reaction kinetics is not limited by the internal resistances to the mass transfer.

3.3. Thermal stability and reusability of the zirconia-entrapped lipase

In order to analyse the stabilizing effect of the immobilisation procedure, the activity-time profiles of both the zirconia-entrapped lipase and the free lipase have been measured at different temperatures (Fig. 6). The experimental data demonstrate the stabilising effect produced by the enzyme entrapment.

The free lipase activity is strongly affected by the temperature. In fact, in 5 days at 30 °C the residual activity fraction is about 0.5, while this decays to 0.1 at 50 °C. Upon increasing the time, essentially complete deactivation occurs at each temperature.

By contrast, the activity of entrapped lipase is reduced only 30–40% after 5 days at 30–50 °C and keeps the residual activity constant for many days whatever the temperature adopted.

Reusability tests were also carried out, to test the stability of entrapped lipases under the storage conditions. After 10 repeated batch tests, the activity of the entrapped lipase was nearly 15% lower than its initial value (data not shown).

3.4. Modelling of the inactivation mechanism

The simplest possible model to describe the enzyme inactivation mechanism is based on the irreversible transition from the native form of the lipase (N) to a completely inactivated form (D), with first order kinetics:

$$N \xrightarrow{k} D \quad (1)$$

In this case, the activity-time profiles are described by a simple exponential expression (see Appendix A):

$$a(t) = a_N e^{-kt} \quad (1')$$

where a_N is the catalytic activity of the native enzyme, and k is the first order kinetic constant. However, as shown in the Fig. 6, the stability tests carried out with free lipase yield convex ln(activity) vs. time curves, according to a double-exponential curve:

$$a(t) = Ae^{-kt} + Be^{-k_2 t} \quad (2')$$

suggesting a departure of the enzyme inactivation kinetics from first order. A mechanistic approach that attaches a physical meaning to the mathematical model (2′) is based on two sequential first order transitions from the native form of lipase (N) to a partially inactivated form (X), and subsequently to a completely inactivated form (D), as shown in the Appendix A:

$$N \xrightarrow{k_1} X \xrightarrow{k_2} D \quad (2)$$

The experimental data in Fig. 6 have been successfully interpolated using Eq. (2′), and the interpolation curves are reported in the same figure.

As regards the lipase immobilised in zirconia, the inactivation profiles (Fig. 6) reach a horizontal asymptote, corresponding to about 60% of the initial value. In this case, the hypothesis can be made that the partially inactivated form of the enzyme (X) does not undergo further modifications. In other words, a simpler form of the mechanism (2) may be considered, assuming $k_2 = 0$:

$$N \xrightarrow{k_1} X \quad (3)$$

corresponding to the following mathematical expression of the inactivation profile:

$$a(t) = Ae^{-k_1 t} + B \quad (3')$$

In synthesis, the stabilising effect of the immobilisation method carried out can be explained assuming that the partially inactivated form of the enzyme, named X in models (2) and (3), is highly stable when lipases are immobilised in zirconia sol–gel, whereas it undergoes further inactivation when the enzyme is not immobilised.

4. Conclusions

This study showed that the lipase entrapment in a zirconia-based sol–gel material can be carried out, to obtain an active catalyst with highly improved stability. Thanks to the higher hydrolysis and polycondensation rates offered by zirconia precursors, the enzyme incapsulation was carried out in the absence of acid or basic catalysts, to reduce the enzyme inactivation. The structural analysis showed that the zirconia matrix was substantially unaffected by the presence of the lipase.

The relative abundance of mesopores reduced the effect of internal diffusional resistances on the catalytic activity of lipases. As a matter of fact, the activation energy of immobilised lipases was not significantly different from that pertaining to the free enzyme. The entrapment increased the thermal stability and the reusability of the lipase, leading to a stable, though partially inactivated, form of the enzyme.

These data support further developments of this methodology, for the immobilisation of lipases or other enzymes of practical interest.

Appendix A

A.1. Model 1: Direct transition from the native form N to a fully inactivated form D

$$N \xrightarrow{k} D$$

if the inactivation kinetics is I order respect to native enzyme concentration:

$$\frac{d[N]}{dt} = -k[N]$$

Upon integration, assuming as initial condition [N] = [N]0:

$$[N] = [N]_0 e^{-kt}$$

As a consequence, the specific activity of the enzyme will be:

$$a = \frac{a_N[N]}{[N]_0} = a_N e^{-kt}$$

A.2. Model 2: Two sequential transitions, considering a partially inactivated form of the enzyme X

$$N \xrightarrow{k_1} X \xrightarrow{k_2} D$$

if both transitions are I order kinetics:

$$\frac{d[N]}{dt} = -k_1[N]$$

$$\frac{d[X]}{dt} = k_1[N] - k_2[X]$$

Upon integration, assuming as initial conditions [N] = [N]0 and [X]0 = 0:

$$[N] = [N]_0 e^{-k_1 t}$$

$$[X] = \frac{[N]_0 k_1}{k_1 - k_2}(e^{-k_2 t} - e^{-k_1 t})$$

As a consequence, the specific activity of the enzyme will be:

$$a = \frac{a_N[N] + a_X[X]}{[N]_0} = \left(a_N - \frac{a_X k_1}{k_1 - k_2}\right) e^{-k_1 t} + \frac{a_X k_1}{k_1 - k_2} e^{-k_2 t}$$
$$= Ae^{-k_1 t} + Be^{-k_2 t}$$

References

[1] A.R. Wilson, P.F. Turner, Biosens. Bioelectron. 7 (1992) 165.
[2] M.T. Reetz, P. Tielmann, W. Wiesenhofer, W. Konen, A. Zonta, Adv. Synth. Catal. 345 (2003) 717.
[3] J. Livage, T. Coradin, C. Roux, in: P. Gomez Romero, C. Sanchez (Eds.), Functional Hybrid Materials, Wiley VCH, Weinheim, 2004, (Chapter 7).
[4] C. Sanchez, B. Julian, P. Belleville, M. Popall, J. Mater. Chem. 15 (2005) 3559.
[5] C.M.F. Soares, O.A. dos Santos, H.F. de Castro, F.F. de Moraes, G.M. Zanin, J. Mol. Catal. B: Enzyme 39 (2006) 69–76.
[6] H.J. Kim, S.H. Yoon, H.N. Choi, Y.K. Lyu, W.Y. Lee, Bull. Korean Chem. Soc. 27 (2006) 65.
[7] J.D. Goud, P.M. Raj, R. Narayan, M. Iyer, R. Tummala, Electronic Components and Technology Conference, Sparks, Nevada, 2007.
[8] V.M. Balcão, A.L. Paiva, F.X. Malcata, Enzyme Microb. Technol. 18 (1996) 392.
[9] Z.D. Knezevic, S.S. Siler-Marinkovic, L.V. Mojovic, APTEFF 35 (2004) 151.
[10] B. Joseph, P.W. Ramteke, G. Thomas, N. Shrivastava, Biotechnol. Mol. Biol. 2 (2007) 39.
[11] F. Kartal, A. Kilinç, S. Timur, Int. J. Environ. Anal. Chem. 87 (2007) 715.
[12] S. Setzu, S. Salis, V. Demontis, A. Salis, M. Monduzzi, M. Mula, Phys. Stat. Sol. A 204 (2007) 1434.
[13] U. Drechsler, N. Fischer, B.L. Frankamp, V.M. Rotello, Adv. Mater. 16 (2004) 271–273.
[14] Y. Nagasaki, K. Yoshinaga, K. Kurokawa, M. Iijima, Colloid Polym. Sci. 285 (2007) 563.
[15] H. El-Rassy, S. Maury, P. Buisson, A.C. Pierre, J. Non-Cryst. Sol. 350 (2004) 23.
[16] S. Maury, P. Buisson, A. Perrard, A.C. Pierre, J. Mol. Catal. B: Enzyme 32 (2005) 193.
[17] A. Galarneau, M. Mureseanu, S. Atger, G. Renard, F. Fajula, New J. Chem. 30 (2006) 562–571.
[18] M. Reetz, Methods in Biology, vol. 22, Humana Press, 2006, p. 65.
[19] O.H. Lowry, N.J. Rosbrough, A.L. Farr, R.J. Randall, J. Biol. Chem. 193 (1951) 265.
[20] F. Rouquerol, J. Rouquerol, K. Sing, Adsorption by powders and porous solids principles, in: Methodology and Applications, Elsevier B.V., 1999.
[21] A. Aronne, P. Pernice, A. Marotta, J. Mater. Sci. Lett. 10 (1991) 1136.
[22] P. Egger, S. Dirè, M. Ischia, R. Campostrini, J. Therm. Anal. Calorim. 81 (2005) 407–415.
[23] M.M. Rashad, H.M. Baioumy, J. Mater. Proc. Technol. 195 (2008) 178–185.
[24] J.A. Bosley, J.C. Clayton, Biotechnol. Bioeng. 43 (1994) 934–938.
[25] H.P. Humphrey, P.A. Wright, J. Mater. Chem. 15 (2005) 3690–3700.
[26] J. He, Z. Song, H. Ma, L. Yang, C. Guo, J. Mater. Chem. 16 (2006) 4307–4315.